NOTES

Radiation Properties and Emissivity Parameterization of High Level Thin Clouds

MAN-LI C. WU

Goddard Laboratory for Atmospheric Sciences, NASA/Goddard Space Flight Center, Greenbelt, MD 20771

18 December 1983 and 30 April 1984

ABSTRACT

To parameterize emissivity of clouds at 11 μm, a study has been made in an effort to understand the radiation field of thin clouds. The contributions to the intensity and flux from different sources and through different physical processes are calculated by using the method of successive orders of scattering.

The effective emissivity of thin clouds is decomposed into the effective absorption emissivity, effective scattering emissivity, and effective reflection emissivity. The effective absorption emissivity depends on the absorption and emission of the cloud; it is parameterized in terms of optical thickness. The effective scattering emissivity depends on the scattering properties of the cloud; it is parameterized in terms of optical thickness and single scattering albedo. The effective reflection emissivity follows the similarity relation as in the near infrared cases. This is parameterized in terms of the similarity parameter and optical thickness, as well as the temperature difference between the cloud and ground.

1. Introduction

The need for a better understanding and parameterization of the radiative properties of cirrus cloud has been appreciated for some time. High level ice clouds are one of the most extensive cloud types in the atmosphere. The radiative properties of thin clouds influence not only the energy balance of climate models, but also the dynamic circulation of the atmosphere. Most of the existing radiation models in climate studies do not treat the emissivity of thin clouds properly, in that almost all of the clouds are treated as blackbodies. One of the reasons for the simple treatment is due to the difficulty and complexity of appropriate methods. The present study is aimed at developing a better treatment for nonblack, thin clouds. In addition, a better understanding of the radiative properties of thin clouds can help in the interpretation of radiometric measurements of surface properties by remote sensing.

Several authors (e.g., Stephens, 1980a; Platt and Stephens, 1980; Cogley and Bergstrom, 1979; Bergstrom and Cogley, 1979; and Liou, 1974; etc.) have studied the radiative properties of cirrus clouds. Liou (1974), using a 16-stream discrete ordinates method, has shown that the radiative properties of cirrus clouds depend strongly upon the particle size distribution. For a fixed thickness, the emissivity depends on the particle concentration and cloud temperature. Cogley and Bergstrom (1979) and Bergstrom and Cogley (1979), using the invariant imbedding method, having investigated the intensity field of the thin clouds from a remote sensing point of view. The upward intensity depends on the single scattering albedo and asymmetry factor for a fixed cloud optical thickness. Platt and Stephens (1980), using a detailed multiple-scattering radiative transfer model based on the discrete space theory, have studied the radiative properties of cirrus clouds. They have shown that the 11 μm flux emittance is quite different from the beam absorption emittance. However, none of them have provided a satisfactory parameterization for the cloud emissivity. The present study is aimed at understanding the details of the radiative properties of thin cloud and in searching for a way to parameterize them. The 11 μm thermal window region is chosen for the present study. This window has been used for the study of the radiative properties of thin cirrus for quite a long time. Stephens (1980a) has also shown that there is a good relationship between the narrow band and broad band emissivities.

To parameterize the emissivity of clouds, an effort has been taken to understand the radiative properties of thin clouds. The contributions to the upwelling and downwelling intensities from various sources and through various physical processes are studied. Cogley and Bergstrom (1979) decomposed the exiting intensities into two components: the intensity arising from *direct* transmission from the distribution of thermal sources, and the *diffuse* intensity arising from space convolutions of the thermal scattering functions that characterize scattering out of a general finite medium. The direct term represents the absorption and emission properties of the medium. The diffuse term represents the thermal scattering properties of the medium. The invariant imbedding method was used in their study.

In the present study, the contributions to the upwelling and downwelling intensities are also separated into direct and diffuse components. There are

Unauthenticated | Downloaded 07/30/21 07:31 PM UTC

direct contributions from the ground due to cloud absorption, diffuse contributions from the ground due to cloud scattering, direct contributions from the cloud due to cloud emission, and diffuse contributions from the cloud due to cloud scattering. The method of successive orders of scattering is used in the present study.

Platt and Stephens (1980), in their study of the high level cloud emittance, decomposed the effective emissivity into effective absorption emissivity, effective scattering emissivity and effective reflection emissivity. They use the method of discrete space theory. Following them, we are also decomposing the effective emissivity into three emissivities. Each emissivity has its own physical meaning and depends on different radiation parameters. A parameterization scheme is searched and developed based on each emissivity's own physical meanings and radiative properties.

2. Radiative transfer model

The axially symmetric radiative transfer equations in thermal infrared, for a plane-parallel atmosphere in local thermodynamic equilibrium can be written as

$$\mu \frac{dI_\nu(\delta, \mu)}{d\delta} = I_\nu(\delta, \mu) - \frac{\omega_\nu}{2}\int_{-1}^{1} P_\nu(\mu, \mu')I_\nu(\delta, \mu')d\mu' - (1 - \omega_\nu)B_\nu, \quad (1)$$

where I_ν represents the monochromatic intensity at the frequency ν, δ the optical thickness, μ the emergent angle with respect to zenith (positive denotes upward direction, negative downward direction, B_ν the Planck function, $P_\nu(\mu, \mu')$ the axially symmetric phase function, and ω_ν the single scattering albedo. For convenience, the subscript ν will be dropped in subsequent discussions.

Equation (1) can be separated into two components: a contribution from the source below the cloud, and a contribution from the internal source of the cloud itself.

a. Contribution from the source below the cloud base

Here

$$\mu \frac{dI_b(\delta, \mu)}{d\delta} = I_g(\delta, \mu) - \frac{\omega}{2}\int_{-1}^{1} P(\mu, \mu')I_b(\delta, \mu')d\mu', \quad (2)$$

with the boundary conditions

$$I_b(\delta_c, -\mu) = 0,$$

$$I_g(0, \mu) = B(T_g)\tau_g + \int_{\tau_g}^{1} Bd\tau.$$

In these equations, I_b represents the monochromatic intensity driven by the source from the cloud boundary, subscript g denotes ground and b denotes cloud boundary, τ is transmittance, T temperature and δ_c total cloud optical thickness. The optical thickness δ equals zero at cloud base and δ_c at cloud top for the present study.

b. Contribution from the internal source of cloud

The expression is

$$\mu \frac{dI_c(\delta, \mu)}{d\delta} = I_c(\delta, \mu) - \frac{\omega}{2}\int_{-1}^{1} P(\mu, \mu')I_c(\delta, \mu')d\mu' - (1 - \omega)B(T_c), \quad (3)$$

with the boundary conditions

$$I_c(\delta_c, -\mu) = 0,$$

$$I_c(0, \mu) = 0.$$

In these equations, I_c represents the monochromatic intensity driven by the internal source of cloud, and c denotes cloud.

Equations (2) and (3) are integro–differential equations. They can also be written in integral forms

$$I_b(\tau, \mu) = I(\tau_b, \mu) + \int_{\tau_c}^{1} J_b(\tau, \mu)d\tau, \quad (4)$$

$$I_c(\tau, \mu) = \int_{\tau_c}^{1} J_c(\tau, \mu)d\tau + (1 - \omega)\int_{\tau_c}^{1} Bd\tau, \quad (5)$$

with

$$J_b(\tau, \mu) = \frac{\omega}{2}\int_{-1}^{1} P(\mu, \mu')I_b(\tau, \mu')d\mu',$$

$$J_c(\tau, \mu) = \frac{\omega}{2}\int_{-1}^{1} P(\mu, \mu')I_c(\tau, \mu')d\mu',$$

$$I(\tau_b, \mu) = I_b(0, \mu).$$

Equations (4) and (5) indicate that when the attenuation due to absorption is small, most of the upward intensity at cloud top originates from the irradiance at cloud base, and little from cloud emission. On the other hand, if absorption is strong, cloud emission and scattering dominate.

The above equations are solved by using the method of successive orders of scattering. The concept of this method is simple. If one knows the origin of sources, one can find how it is distributed through absorption and emission, and where and how it is scattered for the first time. With this as an input, and repeating the process, one can determine the intensity distribution of the second-order scattered photons, and so on. Finally, one can sum all orders of scattering to obtain the total contribution to the radiation field. In the thermal infrared, the single scattering albedo ω is

Unauthenticated | Downloaded 07/30/21 07:31 PM UTC

much less than unity and the convergence of the series will not be a problem.

In numerical applications, the direction integrations are approximated by quadrature formula. The directions are chosen from a set of Gaussian quadrature points such that the direction μ (between 0 and 1) is divided into m-streams (or directions) with a set of associated quadrature weights. The upward and downward fluxes are also approximated by the same set of Gaussian quadrature points. Numerical results indicate that using 16 Gaussian quadrature points or 16 streams with 8 streams in the upward direction and 8 streams in the downward direction is a good approximation. Liou (1974) and Stephens (1980a) also use 16 points in their radiative transfer calculations.

Because the scattering phase functions for realistic ice crystal clouds are still poorly known, the Henyey–Greenstein phase function is used for the present study. For the results presented here, we assume there is one isothermal cloud layer embedded in the atmosphere.

3. Results

In considering the relative importance of direct and diffuse contributions to the radiation field through homogeneous slabs, we present the following discussion and figures. All of the upward and downward intensities and fluxes in the figures have been normalized with respect to irradiances at cloud base. In the present case, it is the ground emitted radiance, because there is no absorption and emission between the cloud and the ground. The optical thickness within the cloud is also normalized to the total cloud optical thickness, which equals unity at the cloud top and zero at the cloud base. The single scattering properties of a polydisperse size distribution of randomly oriented cylinders are taken from Table 1 of Stephens (1980a).

The upward and downward fluxes due to direct contributions, which represent the effect of cloud absorption and emission, are plotted in Figs. 1a and 1b, respectively, for a cloud of optical thickness $\delta_c = 2$. There are two direct contributions to the upward flux. First, the contribution from the ground indicates an exponential decay toward the cloud top due to cloud absorption. For very thin clouds ($\delta_c \sim 0.1$), it decreases linearly toward the cloud top. Second, the direct contribution from cloud, due to cloud emission and absorption, increases toward cloud top. It increases rapidly to its asymptotic limit of $(1 - \omega)B(\tau_c)/B(\tau_g)$ near the cloud top. However, the total direct contribution to upward flux decreases toward the cloud top. It decreases linearly for very thin cloud. For thick cloud it decreases very rapidly (nearly exponentially) in the lower part of the cloud; after it reaches its asymptotic limit, it remains constant toward the cloud top. This indicates that for very thick clouds, the direct contributions from the ground and the lower parts of the cloud to the upward radiance at the cloud top are unimportant, so that the cloud can be treated as blackbody in terms of emission and absorption.

There is only one direct contribution from the cloud to the downward flux because there are no sources above the cloud. This contribution increases nonlinearly to an asymptotic limit of $(1 - \omega)B(T_c)/B(T_g)$ near cloud base, as in the case of the direct cloud contribution to the upward flux. After it reaches its asymptotic limit, the cloud can be treated as a blackbody in terms of emission and absorption. For very thin clouds it increases linearly toward cloud base.

The upward and downward fluxes due to diffuse contributions represent the effect of multiple scattering inside the cloud driven by the thermal source of the cloud and the irradiance at cloud base. These are plotted in Figs. 1d and 1e, respectively. The diffuse upward (downward) flux necessarily equals zero at cloud base (top). The diffuse contribution from the cloud to the upward (downward) flux increases toward cloud top (base). After reaching an asymptotic limit, it remains constant toward cloud top (base). For very thin clouds its contribution to the upward (downward) flux is negligible. The diffuse contribution from the ground to the upward flux initially increases as the optical thickness increases from the base, followed by a decrease toward the cloud top. The level and the magnitude of the maximum depends on the strength of forward scattering as well as the total optical thickness of the cloud. The relative optical thickness level is higher and the magnitude larger for stronger forward scattering. The maximum level is lower for optically thick clouds and the magnitude decreases faster toward the cloud top. It increases linearly toward the cloud top for very thin clouds ($\delta_c \sim 0.1$). The total upward flux follows direct contributions from the ground more rigorously for thin clouds. In the case of thick clouds ($\delta_c \geq 8$), the upward flux more closely follows the diffuse contributions from the ground in the lower portions of clouds and more closely follows the diffuse contribution from cloud in the upper portion of cloud. For a moderate thickness cloud, the total must be treated as a combination of the two. In the downward direction, the diffuse contribution from ground increases toward cloud base. At the base, it may be called the cloud reflection. The cloud reflection is small for thin clouds. It increases rapidly with the total cloud optical thickness, and reaches its asymptotic limit at δ_c of approximately 4.

The total upward, downward and net fluxes are plotted in Fig. 2c. They are the sum of the direct and diffuse contributions. In the case of the upward flux the direct term dominates in the lower portions of the cloud, while the direct and diffuse terms both

Unauthenticated | Downloaded 07/30/21 07:31 PM UTC

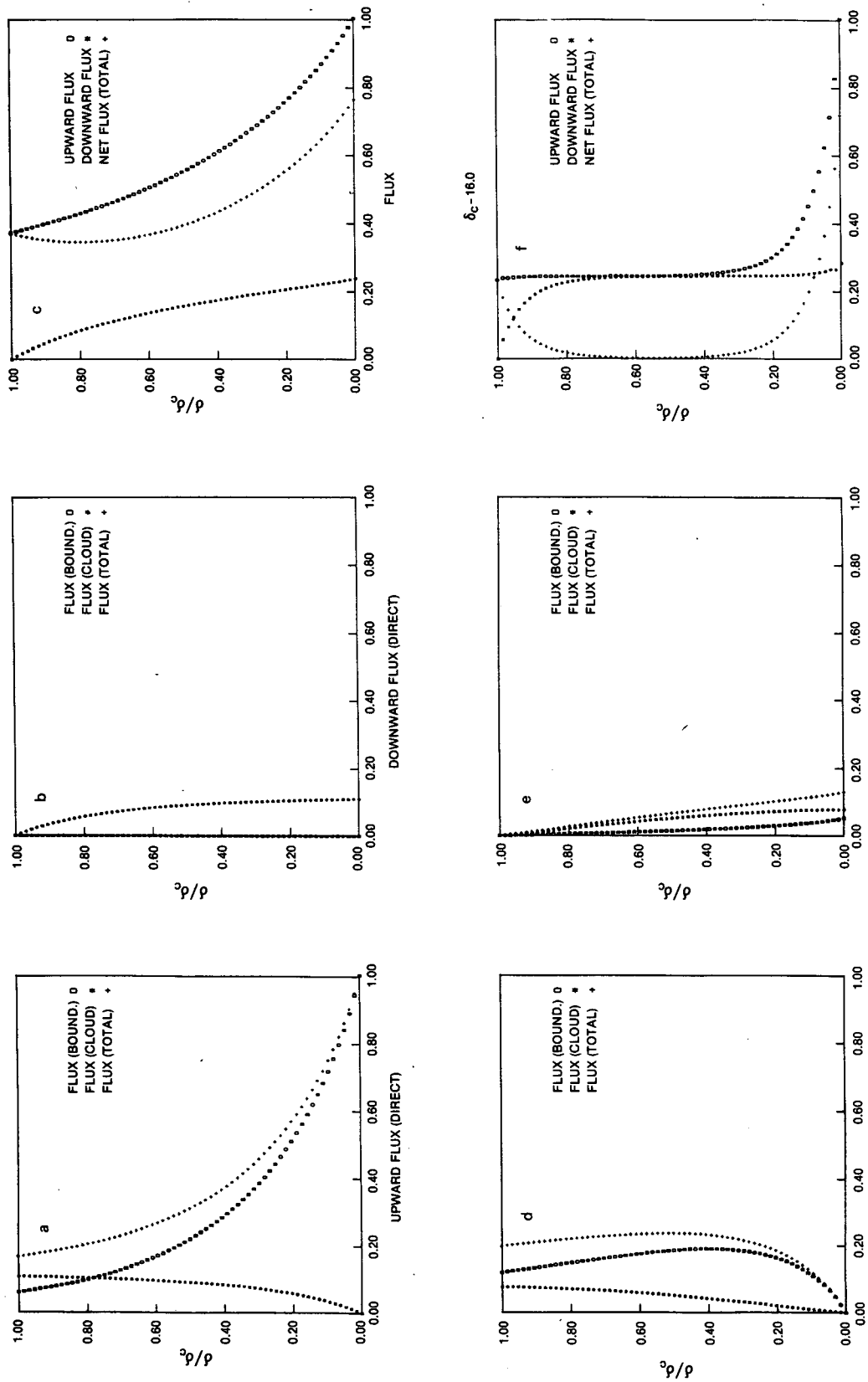

FIG. 1. The upward, downward, and net fluxes: (a) direct contributions to the upward flux; (b) direct contributions to the downward flux; (c) the total upward, downward and net fluxes for δ_c of 2; (d) diffuse contributions to the upward flux; (e) diffuse contributions to the downward flux; (f) the total upward, downward and net fluxes for δ_c of 16.

Unauthenticated | Downloaded 07/30/21 07:31 PM UTC

contribute in the upper portions of the cloud. For very thin clouds the upward flux decreases linearly toward the cloud top; the upwelling radiation at the cloud top is strongly influenced by the ground. For optically thick clouds, the upward flux decreases rapidly in the lower part of the cloud; after it reaches its asymptotic limit, it remains constant toward the cloud top. In this case, the upwelling radiance at the cloud top is the blackbody radiance at the cloud top temperature. The total downward flux increases toward the cloud base. The downward diffuse flux from the cloud contributes more than the cloud reflection terms, except for very thin clouds. The net upward flux is also plotted in Fig. 1c. There is a net radiative warming in the lower portion of the cloud due to the fact that $dF_{net}/d\delta_c < 0$. The warming is due primarily to the hot ground, and is reduced somewhat by cloud reflection. For $\delta_c \geq 2$, there is also radiative cooling in the upper portion of the cloud. The thicker the cloud optically, the greater the cooling. The cooling is due to the absence of thermal sources above the cloud, allowing the cloud to radiate to space, and the ground effect is negligible for optically thick clouds. For thin clouds there is warming at the cloud top. Fig. 1f illustrates the upward, downward and net flux profiles in a cloud of optical thickness $\delta_c = 16$.

The upward and downward intensity at the cloud top and base for a cloud of optical thickness $\delta_c = 2$ are plotted in Figs. 2a and 2b. There is limb darkening in the upward intensity and limb brightening in the downward intensity. The limb brightening is mainly due to the cloud reflection. For thin clouds, the direct contribution to the upward intensity from clouds also contributes to limb brightening. The limb darkening is more complicated to explain, because of the absorption and scattering effect. For very thin clouds, the limb darkening is very strong and it is due mainly to the absorption of direct radiation from the ground. Diffuse contributions from the ground and clouds give limb brightening. For moderate thickness clouds, limb darkening is due mainly to direct and diffuse contributions from the ground (Fig. 2a). For thick clouds ($\delta_c \geq 8$), the limb darkening mechanism is quite reduced, and the darkening is due to diffuse contribution from clouds.

The upward and downward fluxes are plotted in Fig. 3a as a function of total cloud optical thickness. The ground effect decreases as cloud optical thickness increases both for upward and downward directions. In the upward direction, the flux monotonically decreases for an initial value of $\pi B(T_g)$ to an asymptotic limit of $\pi B(T_c)$ as the cloud optical thickness increases to 16 or 32. In the downward direction the flux increases with cloud optical thickness, reaching its asymptotic limit of a cloud optical thickness of 16 or 32.

The flux depends not only on cloud optical thickness, but also on the other radiation parameters, g and ω. The asymmetry factor g, which measures the strength of the forward scattering, ranges from 0.7 to 0.9 for atmospheric clouds. The single scattering albedo, which measures the probability of scattering after a single scattering, ranges from 0.4 to 0.7 in the thermal infrared. The range of these parameters is

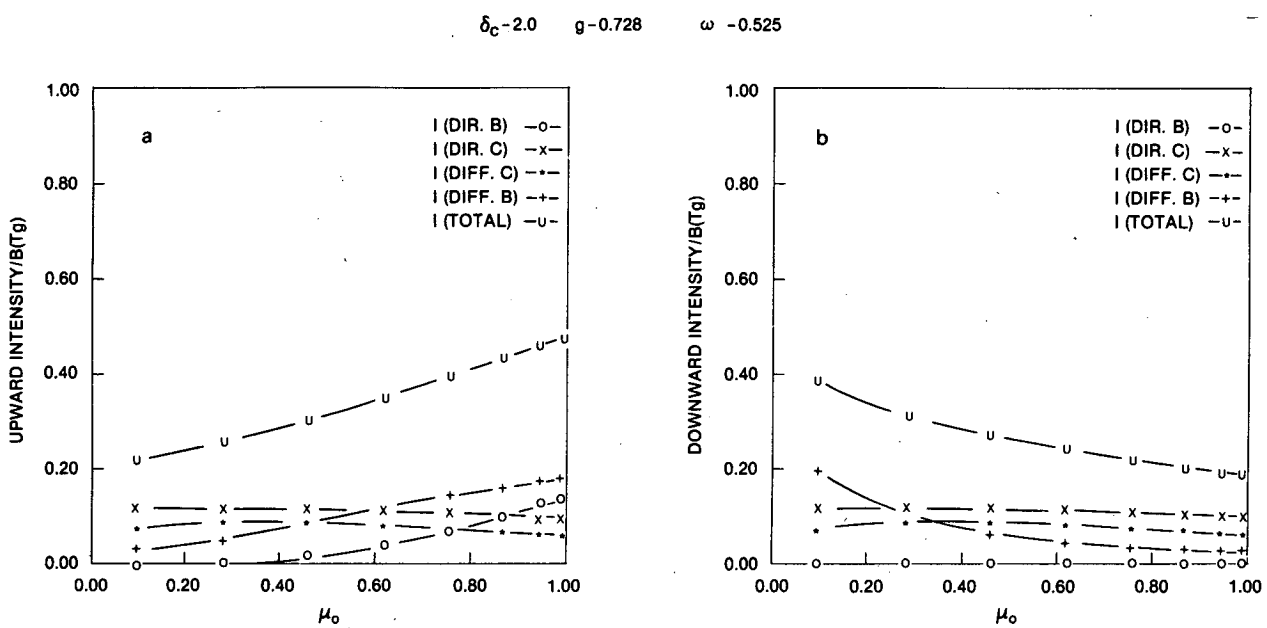

FIG. 2. The upward and downward intensities at cloud top and base as a function of emergent angle: (a) upward intensity; (b) downward intensity.

Unauthenticated | Downloaded 07/30/21 07:31 PM UTC

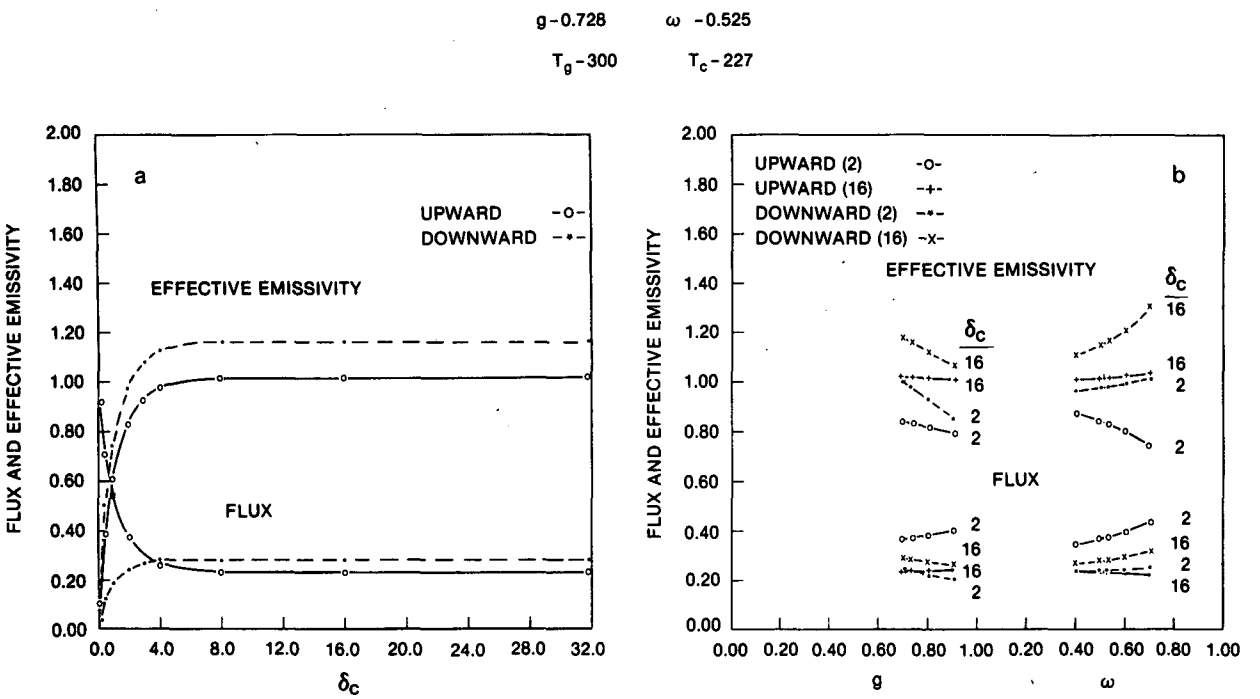

FIG. 3. The upward and downward fluxes and effective emissivities: (a) upward and downward fluxes and effective emissivities as a function of cloud optical thickness, when $g = 0.728$ and $\omega = 0.525$; (b) the upward and downward fluxes and effective emissivities as a function of asymmetry factor (left side of figure) and single scattering albedo (right side of figure).

either commonly known or can be found in Stephens (1980a,b) and Liou (1974). Fig. 3b illustrates the upward and downward fluxes, normalized to the ground blackbody flux $\pi B(T_g)$, and plotted as a function of g and ω for δ_c of 2 and 16.

For $\delta_c = 2$, the upward flux increases with g, due primarily to the stronger forward scattering, which leads to an increase in the diffuse flux arising from the lower boundary. The downward flux decreases with g for the same reason, *viz.*, the diffuse flux from the ground is primarily directed forward (upward), leading to a reduced cloud reflection as g increases.

For $\delta_c = 16$, the upward flux increases very little as g increases, due primarily to the fact that the diffuse contribution to the upward flux from the ground is so little at $\delta_c = 16$. For the downward direction, the flux decreases with increasing g as before, since the increased forward scattering and decreased backward scattering reduces the downward diffuse flux for larger values of g. However, for the downward diffuse flux, the contribution from the ground remains significant at $\delta_c = 16$.

The dependence of the flux on single scattering albedo is also shown in Fig. 3b, The upward flux increases with ω for $\delta_c = 2$. When absorption increases, the contribution from the ground diffuse term decreases, whereas the contribution from cloud emission increases. For thin clouds, the former process dominates, such that the upward flux decreases with increasing absorption. In the downward direction, when absorption increases, cloud emission increases while cloud reflection decreases. In the present case, where $\delta_c = 2$, the cloud reflection term dominates slightly and thus the downward flux increases slightly with ω.

For thick clouds, the ground has very little effect on the upward flux. When absorption increases, cloud emission increases while the cloud thermal scattering effect decreases. If the latter process dominates, the upward flux decreases with ω. In the downward direction, the cloud emission effect and the cloud thermal scattering effect compete with each other. However, the cloud reflection decreases with increasing absorption, so that the downward flux decreases with increasing absorption.

The upward (downward) flux at cloud top (base) depends on several radiation parameters: the asymmetry factor g, the single scattering albedo ω, the cloud optical thickness δ_c and the cloud temperature profile and irradiances at the cloud boundaries. Since it is difficult to parameterize flux, an emissivity approach is used. The concept and usefulness of the effective emissivity has been discussed by Cox (1976). It includes the effect of internal multiple scattering, absorption, emission and reflection. The upward and downward effective emissivities are defined as

$$\epsilon^{\uparrow} = \frac{f_t^{\uparrow} - f_b^{\uparrow}}{\pi B_t - f_b^{\uparrow}}, \quad \epsilon^{\downarrow} = \frac{f_b^{\downarrow} - f_t^{\downarrow}}{\pi B_b - f_t^{\downarrow}}, \tag{6}$$

where $f_t^{\uparrow}$ and $f_b^{\uparrow}$ represent the upward fluxes, $f_t^{\downarrow}$ and

Unauthenticated | Downloaded 07/30/21 07:31 PM UTC

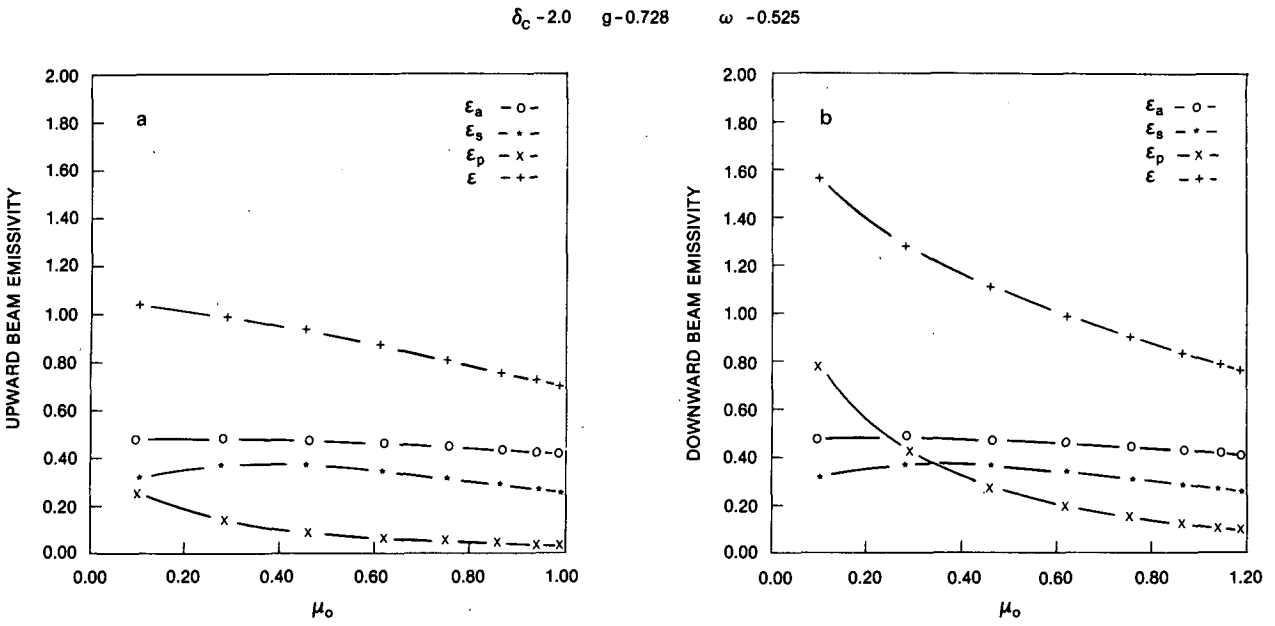

FIG. 4. The effective beam emissivity and its components: (a) the upward effective emissivity and its components as a function of emergent angle; (b) the downward effective emissivity and its components as a function of emergent angle.

$f_b^{\downarrow}$ the downward fluxes, and B_t and B_b the blackbody intensities at cloud top (t) and base (b), respectively.

Following Platt and Stephens (1980), we may further divide the total emissivities into cloud effective absorption emissivities (ϵ_a), scattering emissivities (ϵ_s), and reflection emissivities (ϵ_ρ). Thus, the effective emissivities can be written

$$\epsilon^{\uparrow} = \epsilon_a^{\uparrow} + \epsilon_s^{\uparrow} + \epsilon_\rho^{\uparrow},$$
$$\epsilon^{\downarrow} = \epsilon_a^{\downarrow} + \epsilon_s^{\downarrow} + \epsilon_\rho^{\downarrow}, \quad (7)$$

The effective absorption emissivity depends on the absorption and emission properties within the clouds. The effective scattering emissivity depends on the scattering properties of the clouds. The effective reflection emissivity depends on the reflection properties of the clouds.

Each of these terms is calculated and plotted in Figs. 4a and 4b for the upward and downward effective beam emissivities. For thin clouds, the cloud effective absorption emissivity is larger than that of the cloud effective scattering emissivity in both upward and downward directions. Effective emissivity increases with emergent angle due to cloud reflection, which increases with emergent angle in both directions. For thick clouds, the cloud absorption and scattering emissivities are compatible at small and medium emergent angle. This is because the single scattering albedo is 0.525. When absorption increases, the absorption emissivity will dominate; when absorption decreases, the scattering emissivity will dominate. The upward effective emissivity is almost constant with emergent angle. This is because at large emergent angle, the scattering emissivity decreases while the reflection emissivity increases. These two effects partially cancel one another. In the downward direction, these two effects do not cancel each other very effectively, and the cloud reflection effect dominates. As a consequence, the downward effective emissivity increases markedly with emergent angle.

The total upward and downward effective flux emissivities are plotted in the upper part of Fig. 3a as a function of total cloud optical thickness, and in the upper part of Fig. 3b as a function of g and ω. These figures indicate that the total upward and downward effective flux emissivities are difficult to parameterize.

In the downward direction, the effective emissivity is larger than that in the upward direction because of cloud reflection at the cloud base. For optically thick clouds, this contribution is large. This is the reason for the downward effective emissivity being larger than one.

TABLE 1. Coefficients of polynomials $p(\delta_c)$ and $q(\delta_c)$ for $\epsilon_a/(1-\omega)$.

a	b
−0.579909E3	−0.881144E1
0.859995E3	−0.974618E3
−0.138675E3	0.237239E4
−0.124843E4	−0.206517E4
−0.125606E4	−0.117448E4
1.000000E0	

Unauthenticated | Downloaded 07/30/21 07:31 PM UTC

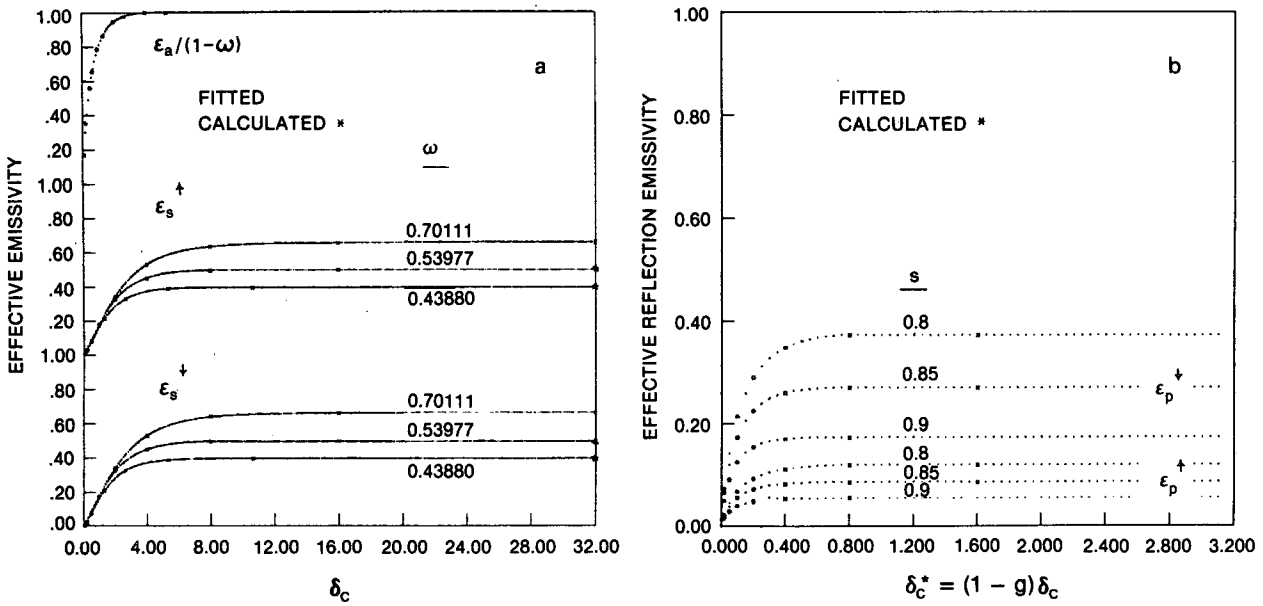

FIG. 5. The component of effective emissivity: (a) the cloud effective absorption emissivity divided by one minus the single scattering albedo as a function of cloud optical thickness at the top of figure; the upward and downward cloud scattering emissivities plotted as a function of cloud optical thickness at middle and bottom of figure; different curve is for different single scattering albedo; (b) the upward and downward effective reflection emissivities as a function of cloud scaled optical thickness; different curve is for different similarity parameter.

4. Parameterization

One way to parameterize the cloud effective emissivity is to parameterize its individual components, because different components have different physical meanings, and therefore depend on different radiation parameters. Fig. 5a is a plot of $\epsilon_a/(1-\omega)$ as a function of cloud optical thickness δ_c. It indicates

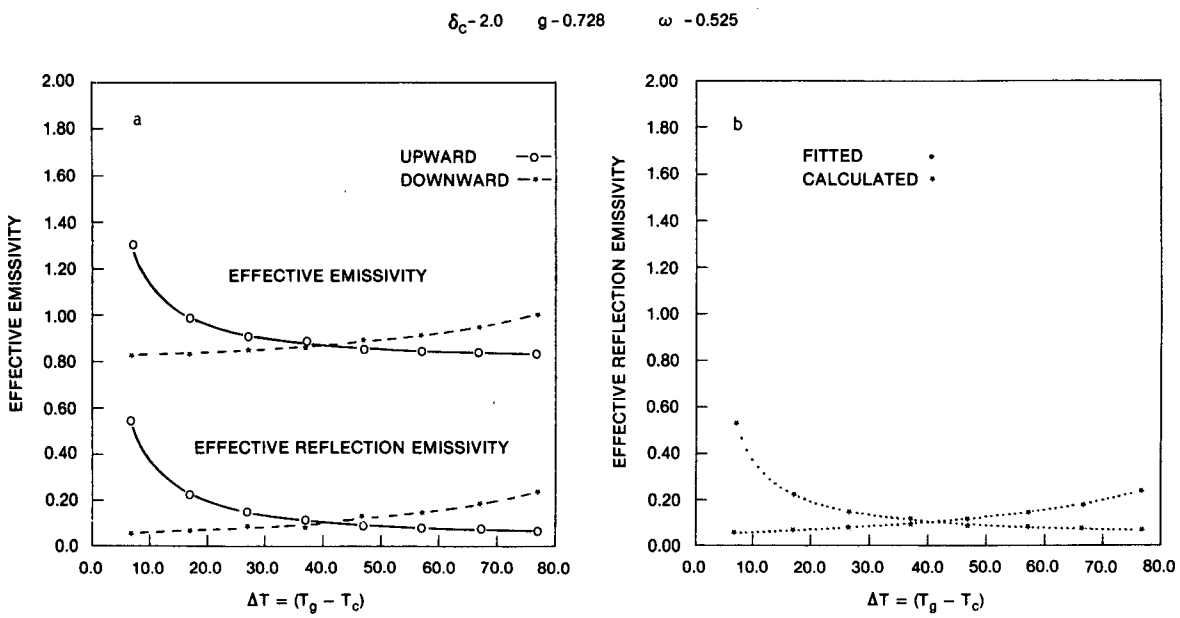

FIG. 6. The upward and downward effective emissivities and effective reflection emissivities as a function of temperature difference between the ground and the cloud. The ground temperature is fixed at T_g = 300 K: (a) the calculated effective emissivity; (b) the fitted emissivity.

Unauthenticated | Downloaded 07/30/21 07:31 PM UTC

TABLE 2. Coefficients of polynomials $p(\delta_c)$ and $q(\delta_c)$ for $\epsilon_s^{\uparrow}$ and $\epsilon_s^{\downarrow}$.

	ω_0					
	0.43880		0.53977		0.70111	
	a	b	a	b	a	b
$\epsilon_s^{\uparrow}$	−0.142793E4	0.367018E2	−0.106300E5	0.363080E2	0.107572E3	−0.10352E1
	−0.275266E3	−0.270547E3	−0.122326E4	−0.174911E4	0.591882E2	0.128347E2
	−0.245565E3	−0.831132E2	−0.926512E3	−0.566231E3	0.352119E2	0.242280E2
	1.000000E0		1.000000E0		1.000000E0	
$\epsilon_s^{\downarrow}$	−0.148586E4	0.354052E2	0.130518E3	−0.194098E1	−0.105265E5	0.123646E2
	−0.276760E3	−0.273906E3	0.642928E2	0.163663E2	−0.109531E3	−0.166014E4
	−0.248049E3	−0.837782E2	0.400795E2	0.266668E2	−0.901599E3	−0.552906E3
	1.000000E0		1.000000E0		1.000000E0	

that $\epsilon_a/(1-\omega)$ depends on δ_c only. It may be parameterized as a ratio of rational function $p(\delta_c)/q(\delta_c)$, where

$$p(\delta_c) = \sum_{i=1}^{N} a_i \delta_c^i,$$

$$q(\delta_c) = \sum_{i=1}^{N} b_i \delta_c^i.$$

Table 1 presents the coefficients a_i and b_i which give the best fit to $\epsilon_a/(1-\omega)$. In Fig. 5a, the asterisks are calculated emissivities while the dots are emissivities computed by these parameterization formula.

The upward and downward cloud scattering emissivities are plotted in the lower part of Fig. 5a as a function of cloud optical thickness. Different curves apply to different single scattering albedos. The cloud reflection emissivity is plotted in Fig. 5b as a function of cloud scaled optical thickness δ_c^* $(=(1-g)\delta_c)$. Two clouds with the same δ_c^* will have approximately the same amount of reflection. Different curves apply to different similarity parameter s, where s combines the effect of single scattering albedo ω and asymmetry factor g and is defined by $s^2 = (1-\omega)/(1-g\omega)$. This similarity parameter equals zero for conservative scattering and increases with increasing absorption; it equals unity for pure absorption or pure forward scattering. In the thermal infrared, the cloud reflection is the only parameter which follows the similarity relation for the range of δ_c we are interested in. Similarity relations were first introduced by van de Hulst and Grossman (1968), and they have been used by others in the visible and near-infrared spectral regions.

The calculated upward and downward effective emissivities are shown in Fig. 6a as a function of temperature difference between the ground and the cloud. The ground temperature is fixed at 300 K. Although the cloud absorption and scattering fluxes depend on cloud temperature, the cloud effective absorption and scattering emissivities do not depend on cloud temperature. The cloud reflection flux does not depend on cloud temperature, but the cloud effective reflection emissivity does depend on cloud temperature. The temperature dependence of the cloud effective emissivity is shown in the lower part of Fig. 6a, which indicates that the temperature dependence of the total effective emissivity is from the cloud effective reflection emissivity. The result of

TABLE 3. Coefficients of $p(\delta_c^*)$ and $q(\delta_c^*)$ for $\epsilon_\rho^{\uparrow}$ and $\epsilon_\rho^{\downarrow}$.

	s					
	0.8		0.85		0.9	
	a	b	a	b	a	b
$\epsilon_\rho^{\uparrow}$	−0.110815E1	0.399451E-2	−0.999684E0	−0.296762E-2	−0.352640E0	0.225148E-2
	−0.775588E1	−0.132170E1	−0.935116E1	−0.107992E1	0.808203E1	−0.564520E0
	0.542922E1	0.103680E1	0.395284E0	0.308103E0	0.376109E2	0.225377E1
	1.000000E0		1.000000E0		1.000000E0	
$\epsilon_\rho^{\downarrow}$	−0.971901E0	−0.103337E1	−0.103000E1	−0.144996E-1	−0.111085E1	−0.122879E-1
	−0.674976E1	−0.363673E1	−0.921924E1	−0.332283E-1	−0.127554E2	−0.277509E1
	−0.675945E1	−0.367277E1	−0.234819E0	0.789051E0	−0.287112E2	−0.442657E1
	1.000000E0		1.000000E0		1.000000E0	

Unauthenticated | Downloaded 07/30/21 07:31 PM UTC

TABLE 4. Coefficients of polynomials $p(\Delta T)$ and $q(\Delta T)$ for ϵ_ρ ($\Delta T = T_g - T_c$) at $\delta_c = 2$, $s = 0.8768$.

$\epsilon_\rho^{\uparrow}$		$\epsilon_\rho^{\downarrow}$	
a	*b*	*a*	*b*
0.146372E5	0.762876E3	0.742546E2	−0.135332E4
−0.227953E3	0.815298E0	−0.397059E3	0.377774E1
1.000000E0		1.000000E0	

fitting as a function of ΔT ($=T_g - T_c$) is plotted in Fig. 6b.

Figure 5 indicates that the components of effective emissivity can be parameterized based on the radiation parameters they depend on. Data are fit to rational functions $p(x)/q(x)$, where the coefficients of polynomials

$$p(x) = \sum_{i=0}^{N} b_i x^i,$$

$$q(x) = \sum_{i=0}^{N} a_i x^i$$

are tabulated in Tables 2 and 3 for the effective scattering and reflection emissivities, respectively, and in Table 4 for the temperature dependence of effective reflection emissivity.

5. Conclusions

Effective emissivity (or flux) is difficult to parameterize because it depends on the radiation parameters in a complicated way (Fig. 3). However, their components, i.e., the effective absorption emissivity, the effective scattering emissivity, and the effective reflection emissivity are easier to parameterize. The effective absorption emissivity depends on the cloud optical thickness only. The effective scattering emissivity depends on the single scattering albedo and cloud optical thickness. The effective reflection emissivity follows the similarity relation, and depends on the scaled optical thickness, similarity parameter and temperature difference between the ground and cloud (Fig. 6). These parameterizations simplify the radiative transfer calculation for nonblack thin clouds. They will be useful not only in climate modeling studies and cloud radiation interaction studies, but also in the remote sensing of cloudtop temperature. The foregoing parameterization is a first step toward this effort.

Acknowledgment. The author is grateful to Drs. Michael D. King and Ming-Dah Chou for their careful review of the manuscript.

REFERENCES

Bergstrom, R. W., and A. C. Cogley, 1979: Scattering of emitted radiation from inhomogeneous and nonisothermal layers. *J. Quant. Spectrosc. Radiat. Transfer,* **21,** 279–292.

Cogley, A. C., and R. W. Bergstrom, 1979: Numerical Results for the thermal scattering functions. *J. Quant. Spectrosc. Radiat. Transfer,* **21,** 263–278.

Cox, S. K., 1976: Observation of cloud infrared effective emissivity. *J. Atmos. Sci.,* **33,** 287–289.

Liou, K. N., 1974: On the radiative properties of cirrus in the window region and their influence on remote sensing of the atmosphere. *J. Atmos. Sci.,* **31,** 552–532.

Platt, C. M. R., and G. L. Stephens, 1980: The interpretation of remotely sensed high cloud emittances. *J. Atmos. Sci.,* **37,** 2314–2322.

Stephens, G. L., 1980a: Radiative properties of cirrus clouds in the infrared region. *J. Atmos. Sci.,* **37,** 435–446.

——, 1980b: Radiative transfer on a linear lattice: Application to anisotropic ice crystal clouds. *J. Atmos. Sci.,* **37,** 2095–2104.

van de Hulst, H. C., and K. Grossman, 1968: Multiple light scattering in planetary atmospheres. *The Atmospheres of Venus and Mars,* J. C. Brandt and M. B. McElroy, Eds., Gordon and Breach, 35–45.

Unauthenticated | Downloaded 07/30/21 07:31 PM UTC